## Title

Synthesis, Stereochemical Analysis, and Derivatization of Myricanol Provide New Probes That Promote Autophagic Tau Clearance



## Journal

ACS Chemical Biology, 10(4)

## ISSN

1554-8929

## Authors

Martin, Mackenzie D
Calcul, Laurent
Smith, Courtney
et al.

## Publication Date

2015-04-17

## DOI

10.1021/cb501013w

Peer reviewed

Published in final edited form as:

*ACS Chem Biol*. 2015 April 17; 10(4): 1099–1109. doi:10.1021/cb501013w.

# Synthesis, Stereochemical Analysis, and Derivatization of Myricanol Provide New Probes That Promote Autophagic Tau Clearance

**Mackenzie D. Martin**[†], **Laurent Calcul**[‡], **Courtney Smith**[‡], **Umesh K. Jinwal**[†], **Sarah N. Fontaine**[†], **April Darling**[†], **Kent Seeley**[‡], **Lukasz Wojtas**[‡], **Malathi Narayan**[†], **Jason E. Gestwicki**[§], **Garry R. Smith**[∥], **Allen B. Reitz**[∥], **Bill J. Baker**[*,‡], and **Chad A. Dickey**[*,‡,†,⊥]

[†]Department of Molecular Medicine and Alzheimer's Institute, University of South Florida, Tampa, Florida 33613, United States

[‡]Department of Chemistry and Center for Drug Discovery and Innovation, University of South Florida, Tampa, Florida 33620, United States

[§]Department of Pharmaceutical Chemistry, University of California, San Francisco, San Francisco, California 94158, United States

[∥]ALS Biopharma, LLC, 3805 Old Easton Road, Doylestown, Pennsylvania 18902, United States

[⊥]James A. Haley Veteran's Hospital, 13000 Bruce B. Downs Boulevard, Tampa, Florida 33612, United States

## Abstract

We previously discovered that one specific scalemic preparation of myricanol (**1**), a constituent of *Myrica cerifera* (bayberry/southern wax myrtle) root bark, could lower the levels of the microtubule-associated protein tau (MAPT). The significance is that tau accumulates in a number of neurodegenerative diseases, the most common being Alzheimer's disease (AD). Herein, a new synthetic route to prepare myricanol using a suitable boronic acid pinacol ester intermediate is reported. An X-ray crystal structure of the isolated myricanol (**1**) was obtained and showed a co-crystal consisting of (+)-a*R*,11*S*-myricanol (**2**) and (−)-a*S*,11*R*-myricanol (**3**) coformers. Surprisingly, **3**, obtained from chiral separation from **1**, reduced tau levels in both cultured cells and *ex vivo* brain slices from a mouse model of tauopathy at reasonable mid-to-low micromolar potency, whereas **2** did not. SILAC proteomics and cell assays revealed that **3** promoted tau degradation through an autophagic mechanism, which was in contrast to that of other tau-lowering compounds previously identified by our group. During the course of structure–activity relationship

[*]**Corresponding Authors:** (B.J.B.) bjbaker@cas.usf.edu., (C.A.D.) cdickey@health.usf.edu.

**Supporting Information**

Figure S1: Synthetic racemic **1** reduces tau levels in a tauopathy cell model with low micromolar potency. Figure S2: LC-MS spectra of **3**-treated cell lysates. Table S1: Top activated and inactivated upstream regulators as determined by IPA software. Table S2: Top canonical pathways as determined by IPA software. Table S3: Upregulated or downregulated kinases as determined by IPA software. Table S4: Crystal data and structure refinement for racemic **2** and **3**. Table S5: Crystal data and structure refinement for enantiopure **2**. Table S6: Results of Bijvoet-pair analysis and Bayesian statistics for enantiopure **2**. Table S7: Crystal data and structure refinement for **13**. Additional experimental methods. This material is available free of charge via the Internet at http://pubs.acs.org.

**Notes**

The authors declare no competing financial interest.

(SAR) development, we prepared compound **13** by acid-catalyzed dehydration of **1. 13** had undergone an unexpected structural rearrangement through the isomyricanol substitution pattern (e.g., **16**), as verified by X-ray structural analysis. Compound **13** displayed robust tau-lowering activity, and, importantly, its enantiomers reduced tau levels similarly. Therefore, the semisynthetic analogue **13** provides a foundation for further development as a tau-lowering agent without its SAR being based on chirality.

## Graphical abstract

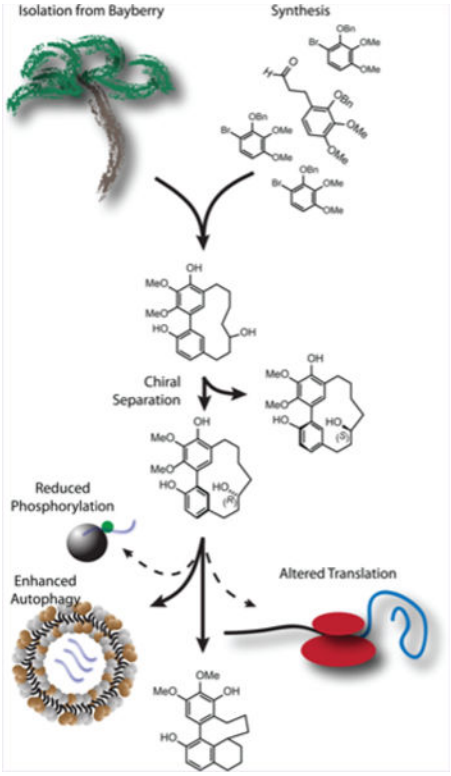


Aberrant accumulation of the microtubule-associated protein tau is implicated in ~20 neurodegenerative disorders, collectively termed tauopathies, including chronic traumatic encephalopathy (CTE), Alzheimer's disease (AD), frontal temporal dementia linked to chromosome 17 (FTDP-17), Parkinson's disease, and Pick's disease.[1,2] Some of these diseases can be caused by mutations in the MAPT gene that result in amino acid substitution in critical microtubule-interacting domains.[3] Tauopathies may also result from a cascade of pathological events, such as amyloid $\beta$ aggregation, leading to microtubule destabilization and the hyperphosphorylation of tau.[4] Tau hyperphosphorylation induces the formation of toxic tau-containing aggregates, resulting in neuronal loss causing cognitive and motor deficits.[5,6]

A number of strategies have been explored to treat tauopathies by targeting mechanisms of tau biology directly. Kinase inhibitors have been used to reduce the hyperphosphorylation of tau and subsequent formation of neurofibrillary tangles. Inhibitors of known tau kinases such as glycogen synthase kinase 3$\beta$ (GSK-3$\beta$), protein kinase C (PKC), Fyn (Src Kinase), and

others have shown decreases in tau pathology.[7] This strategy has had mixed results in the clinic, but none of these inhibitors has been reduced to practice.[8,9] Immunotherapy is another strategy that is being extensively investigated to treat tauopathies. Both active and passive immunotherapy approaches can successfully remove pathological forms of tau in mouse models,[7] but passive immunization holds more promise in the clinic because of its higher selectivity for discrete tau species and greater administrative control in the event of autoimmune reactions. However, even this strategy has some safety concerns since phosphorylated tau species are found in normal as well as AD brains.[10] Nevertheless, clinical trials using passive immunization with antibodies targeting tau are ongoing. Another strategy being explored to treat tauopathies is inhibition of tau aggregation. A number of compounds have been identified that can prevent paired helical filament (PHF) formation and cause PHF disassembly.[7] These compounds have also shown efficacy in mouse models of tauopathy.[11,12] Replacing tau function with microtubule-stabilizing compounds has also shown efficacy in mouse models of tauopathy, and this strategy is currently in the early stages of clinical development.[13] However, currently, there are no approved treatments for the tauopathies that target tau biology directly.[7]

The strategy that our lab has pursued over the past several years is distinct from these other mechanisms in that we are trying to harness the protein quality control machinery to promote tau degradation.[14,15] Molecules targeting heat shock proteins (Hsp), ubiquitin ligase complexes, and deubiquitinating enzymes have been effective at inducing proteasomal degradation of tau.[16] For example, YM-01 and other members of the rhodacyanine family potently inhibit the Hsp70 family of proteins, which concomitantly leads to rapid tau clearance through the proteasome. This scaffold has also been modified successfully to improve brain exposure, suggesting that it could be useful therapeutically.[17] Inhibitors of another chaperone, Hsp90, also have anti-tau activity.[18,19] Like Hsp70 inhibitors, these also facilitate tau degradation via the proteasome. A number of clinical trials have been conducted with Hsp90 inhibitors for other diseases, in particular, cancer, but the success with this approach has been modest due to pharmacological challenges.[20–22] Members of the phenothiazine family, which contains compounds such as methylene blue and azure C, also inhibit Hsp70 protein function, facilitate tau degradation via the proteasome,[15] and rescue memory deficits in tau transgenic mice;[23] however, there is evidence that these compounds also can induce autophagic clearance of tau.[24] Recent work has shown that full-length monomeric tau is most efficiently cleared via the proteasome,[16,25,26] whereas cleaved, oligomeric, and aggregated tau species that are more closely tied to toxicity are more efficiently cleared via autophagy.[16] In fact, autophagic clearance has been shown to be most beneficial in attenuating tauopathies. Activating autophagy with rapamycin was recently shown to have efficacy in a transgenic model of tauopathy,[27,28] potentially ushering in a new avenue for tau-lowering strategies aimed at autophagic pathways. For example, molecules enhancing autophagosome biogenesis and inhibiting the mammalian target of rapamycin (mTOR) both stimulate autophagic tau clearance.[29] Thus, continuing to identify novel small molecules that regulate tau metabolism through these protein clearance pathways could allow us to better understand tau and proteostasis processes as well as serve as a foundation for drug discovery efforts to treat tauopathies.

## RESULTS AND DISCUSSION

We previously showed that a scalemic isolate from myricanol (**1**) (86% ee (+)-a*R*,11*S*-myricanol (**2**)) (Figure 1), a natural product derived from *Myrica cerifera* (bayberry/southern wax myrtle) root bark, lowered tau levels,[30] but the relevance of the stereochemistry and the mechanism through which this occurred remained unknown.[31] One of the obstacles has been to obtain high yields of **2**, and its enantiomer **3**, via synthetic means with completely characterized structure and purity.[32–34] In addition to improving the isolation of **1** from *M. cerifera* root bark,[30] we here devised a novel synthetic route for its production. The first reported synthesis of **1** relied upon the Ni(0)-mediated coupling of a bis-iodide intermediate, in ~10% yield.[32] The synthesis of **1** employed the intramolecular cross coupling of an aryl boronic acid pinacol ester and an aryl iodide, as the boronic acid pinacol ester functionality has been established as a useful partner in macrocycle ring formation.[35] Aryl bromide **4** was converted to phenylpropionaldehyde **5** by palladium-mediated reductive coupling with allyl alcohol (Figure 1). Iodination of **5** proceeded primarily *ortho* to the methoxy group to give **6**, in 76% yield. 4-(4-Benzyloxy)butan-2-one **7** was converted to iodide **8**, which then afforded boronic acid pinacol ester **9**. Intermediate **9** was treated with LDA followed by **6** to effect an aldol condensation to give **10**, after acid-mediated elimination to the *α*,*β*-unsaturated ketone, in 39% overall yield. Intramolecular cyclization of **10** using a palladium catalyst gave desired **11** in 22% yield. We also conducted experiments on related substrates bearing two iodines without the boron acid pinacol ester using Ni(0) catalysts, which had also been reported in the synthesis of the related natural product alnusone[36] but found no improvement over the ~10% yield reported earlier.[32] The olefin was reduced and the benzyl ethers of **11** were removed via hydrogenolysis to give **12**, the reduction of which gave **1** (Figure 1).

*M. cerifera*-derived **1** is a *m*,*m*-bridged diarylheptanoid consisting of the two enantiomers, **2** and **3**, but **2** is in enantiomeric excess (~13:1 ratio).[30] It could also possess the two atropisomers, **2a** and **3a** (Figure 2A). To determine if synthetic **1** had a similar enantiomer composition as that of purified **1**, it was subjected to chiral separation by high-performance liquid chromatography (HPLC), resulting in two UV fraction peaks with identical retention times as those observed for *M. cerifera*-derived **1** but at a 1:1 ratio (Figure 2A,B). Crystal structures were obtained of the racemic purified **1** and the purified enantiomer **2**, allowing us to infer the structure of **3** (Figure 2C,D). Analysis of the solid-state structure shows that the stereochemistry of the hydroxyl group on the macrocyclic ring appears to direct two opposite atropisomer geometries relative to the biphenyl rings, which are highly strained. The internal dihedral angle of the biphenyl is 31.5°, relative to the carbocyclic ring, whereas the external dihedral angle is 45.1°, which means a 13.4° twist in the phenyl rings for the two rings combined. There is a 7-membered ring hydrogen bond between the 5-OH and 4-OMe groups on the biphenyl rings (2.6 Å between non-hydrogen atoms).[37,38]

Previously, we showed that scalemic **1** isolated from *M. cerifera* had anti-tau activity, whereas racemic **1** derived from another source did not.[30] Therefore, we wanted to determine whether synthetic **1** had efficacy against tau similar to that of *M. cerifera*-derived **1**. Indeed, using HEK293T cells stably overexpressing P301L tau (an FTD-causing mutation prone to aggregation; HEK P301L), we confirmed that this newly synthesized **1** did, in fact,

lower tau levels (Supporting Information Figure 1). Also, in our previous work, we hypothesized that **2** was the more abundant chiral isolate from **1** because it was the enantiomer in excess in **1** derived from *M. cerifera*. However, this hypothesis was never confirmed because we did not isolate the enantiomers and analyze their anti-tau efficacy individually. Above, we determined that both synthetic and *M. cerifera*-derived **1** contained only two of the four possible isomers of **1: 2** and **3**. However, *M. cerifera*-derived **1** had a 14:1 ratio of **2** to **3**, whereas synthetic **1** had a 1:1 ratio (Figure 2). Therefore, we sought to determine if these enantiomers each had anti-tau activity or whether one of these was driving the majority of the anti-tau efficacy of **1**. HEK P301L cells were treated with either **2** or **3** over a 72 h time course. Surprisingly, 30 μM **3** decreased both phosphorylated and total tau levels similarly after just 6 h of treatment, and levels were reduced by as much as 50% after 72 h. In contrast, treatment with **2** at 30 μM did not reduce tau levels throughout the duration of the experiment in this cell model (Figure 3A,B) despite previous work showing anti-tau activity at higher concentrations.[30] These surprising results indicated that the chirality of **1**, based on the asymmetric carbon C-11 of the macrocyclic ring, and the biphenyl atropisomerism are indeed essential for the anti-tau activity of **1**, but not as originally predicted based on the enantiomer excess inference.[30] Instead, it is the minor constituent of **1**, **3**, that is responsible for the majority of tau-lowering activity. Therefore, any preparation of racemic **1** that possesses **2** and **3** together should have anti-tau activity, but not all preparations of racemic **1** may lower tau levels because they could possess a different isomer profile.

Our previous interpretation was based on an inference of two racemic mixtures of naturally derived myricanol from two different sources: one from *M. cerifera* and the other from another source not disclosed by Indofine Chemical but that was likely from *Myrica rubra*, which is the typical source. The X-ray data from *M. cerifera*-derived myricanol that we prepared here revealed the presence of only 2 isomers. However, no X-ray data was collected on the racemic material obtained from Indofine Chemical, which possibly possessed a distinct stereoisomer profile. This could be due to environmental or species differences between where the material used here and the material used by Indofine Chemical were harvested and/or the methods used for extracting the natural product. Either modification could result in epimerization of the atropisomers. Also, while in our previous work the chiral column HPLC revealed two peaks in the racemic mixture from Indofine Chemical that appeared similar to the mixture we isolated from *M. cerifera* ourselves, it is likely that the atropisomerism could not be resolved with the column that we used. Another consideration is that the myricanol purchased from Indofine Chemical may have lacked the same purity as the myricanol that we purified. Any of these alterations could possibly explain the lack of activity of the 55:45 racemic preparation used in our previous work. Because of this unexpected result, we were also concerned that **3** was possibly being metabolized in the cell, particularly given its polyphenolic structure. Therefore, we subjected lysates of cells treated with **3** for 1, 6, and 24 h to liquid chromatography mass spectrometry (LC-MS) analysis. Interestingly, the amount of **3** found in cells increased over time, likely due to cell permeability, and, more importantly, there was no metabolite observed (Supporting Information Figure 2). This confirmed that **3** was indeed the active molecule.

We then compared the anti-tau activity of **3** to another well-established tau-reducing compound, YM-01.[39] HEK P301L cells were treated with increasing concentrations of **3** and YM-01 for 24 h (Figure 3C). YM-01 reduced the levels of tau at lower concentrations than **3**, but the difference was slight ($IC_{50}$ = 3 $\mu$M and 18 $\mu$M Figure 3D). We examined whether 24 h **3** treatment reduced the levels of other known tau mutations associated with disease. HEK293T cells were transfected with P301L, wild-type (WT), G303V, V337M, R406W tau species containing all four microtubule binding domains and no N-terminal insertions (4R0N) and were treated with the $IC_{50}$ of either YM-01 (3 $\mu$M) or **3** (18 $\mu$M) for 24 h. While tau levels in most of these mutants were reduced by either treatment, R406W tau was resistant to both compounds (Figure 3E,F). This corroborates previous work showing that this particular tau mutant (R406W) is more resistant to tau-lowering agents, perhaps because of its more hydrophobic structure.[15]

Next, we tested the anti-tau activity of **3** in a more physiologically relevant context, using brain tissue from the rTg4510 mouse model, which overexpresses P301L tau.[40] Acute *ex vivo* brain slices were treated with YM-01 and **3** (Figure 3G) for 6 h.[39,41] These slices can survive only for approximately 6–8 h. Therefore, higher concentrations of treatments are typically used to accelerate manifestation of activity. YM-01 significantly reduced tau levels at 30 and 100 $\mu$M, as previously described.[39] (−)-a*S*,11*R*-Myricanol (**3**) also significantly decreased tau levels in rTg4510 brain slices at higher concentrations (100 and 150 $\mu$M) (Figure 3H). Thus, enantiomer **3** reduced tau levels in both cultured cells and an *ex vivo* model of tauopathy.

We then sought to investigate the kinetics of tau clearance caused by **3** treatment. To do this, we used a previously characterized cell model, the inducible iHEK WT tau cell line.[41] This cell model allows us to monitor the degradation of tau protein exclusively by turning tau expression on and then off using tetracycline and monitoring tau levels after transgene expression is suppressed. To assess how **3** affected tau degradation, iHEK cells were induced to overexpress tau for 24 h, and then tau expression was shut off by removal of the tetracycline. Cells were then treated with **3** over 24 h. After 6 and 24 h, **3** significantly enhanced the temporal clearance of tau protein compared to that in cells treated with vehicle only (Figure 4A,B). This tau-specific chase experiment confirmed that **3** was, in fact, accelerating tau clearance, not regulating its production.

Using this same model, we investigated how **3** was impacting other well-known tau epitopes. Tau expression was induced with tetracycline in iHEK WT tau cells for 24 h and then tetracycline was removed to stop tau expression. Cells were then treated with **3**, and lysates were harvested at the indicated time points. After 1 h, **3** accelerated reductions of tau phosphorylated at S396/S404 and T231 compared to that in cells treated with vehicle alone. Levels of tau phosphorylated at S262 and S356 were unchanged compared to that in vehicle-treated cells, consistent with previous findings that this particular phospho-tau species is resistant to tau-lowering agents[15,18] (Figure 4C,D). The clearance of both total tau species (epitopes were $\alpha\alpha$ 2–18 or 404–441) was accelerated by **3**, but this occurred more slowly than it did for pS396/S404 and T231 tau species. Thus, select phospho-tau species are rapidly reduced by **3** treatment, whereas total tau levels are reduced, but with greater latency.

We previously demonstrated that the tau-lowering compound, YM-01, promoted tau clearance through a ubiquitin-dependent proteasomal mechanism.[39] This is indicated by the accumulation of high molecular weight tau species following treatment with YM-01 in HEK P301L cells (Figure 5A). However, we observed that treating these same cells with **3** did not produce high molecular weight tau (Figure 5B). We also showed previously that YM-01-mediated tau lowering was blocked when cells were cotreated with a proteasomal inhibitor,[39] but treating cells with the proteasomal inhibitor, MG-132, had no impact on the tau-lowering activity of **3** (Figure 5C,D), suggesting that **3** was clearing tau through an alternative non-proteasomal mechanism.

We then turned to an unbiased approach to identify a possible mechanism that was triggered by **3** to facilitate tau clearance. We used SILAC proteomic analysis on lysates of the neuronal cell line (M17) treated with or without **3** to help elucidate its possible mechanism of action. These experiments were performed in triplicate, and data was analyzed using Ingenuity Pathway Analysis (IPA) software. Any peptides represented in only one of these triplicates were excluded from the analysis. To identify which other compound(s) **3** most closely represented, we turned to the top upstream regulator prediction feature of the IPA software. On the basis of our SILAC proteomic results, this feature allowed us to predict those compounds or proteins that activated or inhibited similar pathways as those modulated by **3**. Interestingly, the pathways activated by **3** treatment were the same as those activated by the compound sirolimus/rapamycin (Supporting Information Table 1). Rapamycin is a known autophagy activator and has previously been implicated as a possible treatment for tauopathy.[42,43] On the basis of this insight, HEK P301L tau cells were cotreated with the autophagy inhibitor, 3-methyladenine (3-MA), and **3**. In the absence of 3-MA, **3** reduced tau levels as expected; however, when 3-MA was present, **3** activity against tau was abrogated (Figure 6A,B). Compound **3** also induced LC3$\beta$ in the iHEK cell model (Figure 6C), a protein known to be elevated when autophagy is activated.[44,45] These findings provided further evidence that part of the tau-lowering activity of **3** was due to activation of autophagy.

While **3** most closely resembled activated rapamycin signaling, there were other pathways that were predicted to be somewhat impacted by **3** treatment, albeit to a lesser extent. Some of these pathways could be contributing to the effects of **3** on tau biology. For example, **3** was shown to regulate a variety of translational proteins from the EIF2, EIF4/p70S6K, and mTOR pathways (Supporting Information Table 2). While our data from Figure 4 suggests that impaired translation of tau is not a major contributor to the tau-lowering activity of **3**, it could be having some effect. In fact, we have previously shown that tau itself can alter the EIF2 pathway,[46] further suggesting a link between this mechanism and tau. We also noticed that discrete phospho-tau species were being rapidly reduced by **3** (Figure 4C). The pS396/S404 and pT231 epitopes most affected by **3** (Figure 4C) were those typically phosphorylated by known serine/threonine tau kinases such as glycogen synthase kinase 3$\beta$ (GSK3$\beta$), casein kinase 2 (CK2), and mitogen activated protein kinase 1 (MAPK1/ERK2), as well as members of the protein kinase A family. While the levels of GSK3$\beta$ itself were not directly influenced by **3** according to the proteomic data, an upstream kinase capable of modifying GSK3$\beta$ signaling was, MAPK1/ERK2[47] (Supporting Information Table 3). In

addition, both CK2 and a member of the PKA family were also reduced by **3** treatment (Supporting Information Table 3). This could represent another mechanism through which **3** is regulating tau biology: by decreasing known tau kinases. Overall, while our data suggests that activation of autophagy is the major activity of **3** that promotes tau clearance, our proteomic data provides additional details about other mechanisms through which **3** could modify tau biology.

We then heated **1** in the presence of *p*TsOH for 24 h to try to eliminate the active stereocenters and reduce the OH group at C11. The major product was the cyclized tetralin derivative **13**, in 45% yield (Figure 7A). We were surprised by the observation of this derivative because rather than having the expected *m*,*m*-bridged substitution (compound **14**) pattern the molecule had rearranged to an *o*,*m*-bridge, as determined by X-ray crystallography (Figure 7B), likely because of the relief of ring strain in **1**. The X-ray crystal analysis of B showed the enantiomers of **13** as a*R*,10*R* and a*S*,10*S*, but, after chiral HPLC, no assignment was determined for (+)-**13** and (−)-**13**. Myricanone (**12**) has been reported to rearrange to **15** upon treatment with Lewis acid boron trifluororide ($BF_3$),[48] so we repeated this reaction. Reduction of **15** using sodium borohydride gave **16**, which is reported for the first time (Figure 7A). Interestingly, while compounds **12**, **15**, and **16** were inactive against tau (not shown), compound **13** maintained anti-tau activity that was similar to **3**, despite the rearrangement, alteration of the macrocycle ring, and reduction of the hydroxyl group at C11 (Figure 8A,B). This was important because it suggested that the exposed hydroxyl moieties on the biphenyl motif were not causing tau degradation through a pan-assay interference phenomenon.[49] The enantiomers of **13** were separated and collected individually by chiral HPLC to evaluate whether the chiralities (C10 and 1,19-biphenyl) of **13** were as important for activity as those (C11, 1,2-biphenyl) for **3** were. Both (+)-**13** $\left([\alpha]_{\mathrm{D}}^{20}=+93.6\ (c=0.08, \mathrm{chloroform})\right)$ and (−)-**13** $\left([\alpha]_{\mathrm{D}}^{20}=-100\ (c=0.09, \mathrm{chloroform})\right)$ had similar activity against tau (Figure 8C), suggesting that this molecule maintains anti-tau activity independent of chirality.

In conclusion, we have developed a new synthetic route for the production of **1**. Enantiomer **3** reduced tau levels in several models of tauopathy. This molecule promoted tau clearance by activating autophagy, but SILAC proteomic analysis suggested that other pathways may also be engaged to alter tau production and phosphorylation. We also produced **13**, a derivative of **1**, and both (+) and (−) enantiomers of **13** maintained tau-lowering efficacy. We attributed this to several unique structural features that emerged during the preparation of **13**. This work represents a major step forward in understanding the stereochemistry and biochemistry of this scaffold and perhaps defines **3** and **13** as early stage anti-tau therapeutics and tools for investigating autophagy.

## METHODS

Details regarding chemical synthesis, high-resolution mass spectrometry, crystallographic determinations, and SILAC methodologies are included in the Supporting Information.

All chemicals and anhydrous solvents were purchased from commercially available sources and used without additional purification. General solvents and reagents were purchased from Fisher Scientific. HRMS was performed on JMS-T100LC AccuTOF Reflectron time-of-flight mass spectrometer with ESI source, MS-50010BU TOFMS base unit (resolution, 6000 (fwhm), 5 ppm accuracy of mass value), and Agilent 7980 gas chromatography quadrupole time-of-flight mass spectrometer 7200 series with EI source. $^1$H NMR spectra were obtained on a Varian Mercury 300-MHz NMR and Varian 500-MHz NMR DD cryoprobe. Chemical shifts are reported in parts per million (ppm, $\delta$) using various solvents as internal standards ($CDCl_3$, $\delta$ 7.26; DMSO-$d_6$, $\delta$ 2.50). $^1$H NMR splitting patterns were designated as singlet (s), doublet (d), triplet (t), or quartet (q). Splitting patterns that could not be interpreted or easily visualized are recorded as multiplet (m) or broad (br). Coupling constants were reported in hertz (Hz). Purity (%) and mass spectral data were determined with a Waters Alliance 2695 HPLC/MS (Waters Symmetry C18, 4.6 × 75 mm, 3.5 $\mu$m) equipped with a 2996 diode array detector from 210–400 nm; the solvent system is 5–95% acetonitrile in water with 0.1% TFA over 9 min using a linear gradient. The chiral separation was performed with a Shimadzu 10AT HPLC (Phenomenex Lux Cellulose-1, 10 × 250 mm, 5 $\mu$m) equipped with a SPD-10Av detector at 254 nm. Isocratic solvent system 1 was 5% isopropanol in hexane, and isocratic solvent system 2 was 3% isopropanol in hexane at a flow rate of 5 mL min$^{-1}$; retention times are in minutes.

## Reagents

YM-01 was provided by J. Gestwicki. MG-132 was obtained from AG Scientific and 3-MA was obtained from Sigma-Aldrich. 3-MA was solubilized in water to 0.2 M. All other compounds were solubilized in DMSO (Sigma-Aldrich) to 30 mM. Lipofectamine 2000 from Invitrogen was used for all transfections.

## Cell Culture

HEK293T (ATCC) cells stably expressing P301L 4R0N tau, BE(2)-M17 (ATCC) cells, and HEK293T cells were maintained in DMEM plus 10% FBS (Life Technologies), 1% penicillin– streptomycin (Invitrogen), and 1% Glutamax (complete media; Thermo Scientific). HEK293T cells stably overexpressing tetracycline-regulatable WT Tau 4R0N were maintained under zeocin and blasticidin S HCl (Invitrogen) selection in complete DMEM. HeLa (ATCC) cells stably expressing V5-tagged 4R0N tau[15] were maintained under G418 selection in Opti-Mem plus 10% FBS (complete media; Invitrogen) as previously described.[15] Transfections were performed following Invitrogen's plasmid DNA transfection protocol using Opti-MEM. All cells were treated as indicated and were harvested as previously described.[15] Cells were washed twice in ice-cold PBS and then scraped in cold MPER (Fisher Scientific) containing protease and phosphatase inhibitors (PIC III, Calbiochem, PI2 and PI3, Sigma, PMSF). Samples were allowed to incubate on ice, vortexed, and then centrifuged at 10 000 rpm for 5 min at 4 °C to clear debris.

## *Ex Vivo* Slice Cultures

All procedures involving experimentation on animal subjects were done in accordance with the guidelines set forth by the Institutional Animal Care and Use Committee of the

University of South Florida. Male 4 month old rTG4510 slice cultures were treated and maintained as previously described.[30]

### Western Blotting

After normalization of protein concentration by bicinchoninic acid (BCA) (ThermoFisher), samples were run on 10% SDS-PAGE gels and transferred to PVDF (Immobilon, EMD Millipore). Membranes were blocked for 1 h in 7% nonfat dry milk in TBS-T before probing with anti-tau antibodies H150 (Santa Cruz Biotechnology) and pT231 (Anaspec). Anti-actin and anti-GAPDH were purchased from Sigma-Aldrich and Biodesign. All antibodies were used at a dilution of 1:1000. Anti-S396/S404 phosphorylated tau antibody (pS396/404) was used at a dilution of 1:500 (provided by P. Davies). Primary antibodies were decteced by the species-appropriate secondary antibodies (Southern Biotech). Antibodies were detected by ECL (ThermoFisher).

### Densitometry (Quant)

All values are shown as percent vehicle following actin normalization ± standard error of the mean. Scion Image software was used to calculate densitometry of all western blots.

### SILAC/Proteomic Analysis

M17 neuroblastoma cells were labeled for quantitation using SILAC media supplemented with 10% dialyzed FBS, pen/strep, and L-lysine or $^{13}C_6$-L-lysine 2HCl for M17 neuroblastoma cells (Thermo Scientific). Cells were maintained in T25 flasks, and the subsequent procedure was followed as previously described.[50] SILAC-fed neuronal M17 cells were treated with **3** or vehicle for 72 h. Quantification was done using Ingenuity Pathway Analysis software. The experiment was performed in triplicate. Proteins without peptide representation in at least two of the triplicates were excluded from the analysis.

### Statistics

Statistical analyses were performed by one-way ANOVA tests or Student's *t* tests.

## Supplementary Material

Refer to Web version on PubMed Central for supplementary material.

## Acknowledgments

Funding for this work was provided by the National Institutes of Health (AG044956 and NS073899 C.A.D.) and Veteran's Health Administration (BX001637 C.A.D.). We would like to thank G. Caldwell of Johnson & Johnson for helpful discussion and analysis. This material is the result of work supported with resources and the use of facilities at the James A. Haley Veterans' Hospital. The contents of this publication do not represent the views of the Department of Veterans Affairs or the United States Government. A Florida Center of Excellence grant to USF provided the resources of the Center for Drug Discovery and Innovation.

## References

1. Hardy J, Orr H. The genetics of neurodegenerative diseases. J Neurochem. 2006; 97:1690–1699. [PubMed: 16805777]

2. McKee AC, Cantu RC, Nowinski CJ, Hedley-Whyte ET, Gavett BE, Budson AE, Santini VE, Lee HS, Kubilus CA, Stern RA. Chronic traumatic encephalopathy in athletes: progressive tauopathy after repetitive head injury. J Neuropathol Exp Neurol. 2009; 68:709–735. [PubMed: 19535999]
3. Spillantini MG, Goedert M. Tau pathology and neurodegeneration. Lancet Neurol. 2013; 12:609–622. [PubMed: 23684085]
4. Lee VM, Goedert M, Trojanowski JQ. Neurodegenerative tauopathies. Annu Rev Neurosci. 2001; 24:1121–1159. [PubMed: 11520930]
5. Iqbal K, Alonso AD, Gondal JA, Gong CX, Haque N, Khatoon S, Sengupta A, Wang JZ, Grundke-Iqbal I. Mechanism of neurofibrillary degeneration and pharmacologic therapeutic approach. J Neural Transm, Suppl. 2000; 59:213–222. [PubMed: 10961432]
6. Ramsden M, Kotilinek L, Forster C, Paulson J, McGowan E, SantaCruz K, Guimaraes A, Yue M, Lewis J, Carlson G, Hutton M, Ashe KH. Age-dependent neurofibrillary tangle formation, neuron loss, and memory impairment in a mouse model of human tauopathy (P301L). J Neurosci. 2005; 25:10637–10647. [PubMed: 16291936]
7. Gerson JE, Castillo-Carranza DL, Kayed R. Advances in therapeutics for neurodegenerative tauopathies: moving toward the specific targeting of the most toxic tau species. ACS Chem Neurosci. 2014; 5:752–769. [PubMed: 25075869]
8. Nygaard HB, van Dyck CH, Strittmatter SM. Fyn kinase inhibition as a novel therapy for Alzheimer's disease. Alzheimers Res Ther. 2014; 6:8. [PubMed: 24495408]
9. Piette F, Belmin J, Vincent H, Schmidt N, Pariel S, Verny M, Marquis C, Mely J, Hugonot-Diener L, Kinet JP, Dubreuil P, Moussy A, Hermine O. Masitinib as an adjunct therapy for mild-to-moderate Alzheimer's disease: a randomised, placebo-controlled phase 2 trial. Alzheimer's Res Ther. 2011; 3:16. [PubMed: 21504563]
10. Blair LJ, Nordhues BA, Hill SE, Scaglione KM, O'Leary JC III, Fontaine SN, Breydo L, Zhang B, Li P, Wang L, Cotman C, Paulson HL, Muschol M, Uversky VN, Klengel T, Binder EB, Kayed R, Golde TE, Berchtold N, Dickey CA. Accelerated neurodegeneration through chaperone-mediated oligome-rization of tau. J Clin Invest. 2013; 123:4158–4169. [PubMed: 23999428]
11. Congdon EE, Figueroa YH, Wang L, Toneva G, Chang E, Kuret J, Conrad C, Duff KE. Inhibition of tau polymerization with a cyanine dye in two distinct model systems. J Biol Chem. 2009; 284:20830–20839. [PubMed: 19478088]
12. Ballatore C, Crowe A, Piscitelli F, James M, Lou K, Rossidivito G, Yao Y, Trojanowski JQ, Lee VM, Brunden KR, Smith AB III. Aminothienopyridazine inhibitors of tau aggregation: evaluation of structure–activity relationship leads to selection of candidates with desirable *in vivo* properties. Bioorg Med Chem. 2012; 20:4451–4461. [PubMed: 22717239]
13. Brunden KR, Trojanowski JQ, Lee VM. Advances in tau-focused drug discovery for Alzheimer's disease and related tauopathies. Nat Rev Drug Discovery. 2009; 8:783–793. [PubMed: 19794442]
14. Blair LJ, Zhang B, Dickey CA. Potential synergy between tau aggregation inhibitors and tau chaperone modulators. Alzheimer's Res Ther. 2013; 5:41. [PubMed: 24041111]
15. Jinwal UK, Miyata Y, Koren J III, Jones JR, Trotter JH, Chang L, O'Leary J, Morgan D, Lee DC, Shults CL, Rousaki A, Weeber EJ, Zuiderweg ER, Gestwicki JE, Dickey CA. Chemical manipulation of hsp70 ATPase activity regulates tau stability. J Neurosci. 2009; 29:12079–12088. [PubMed: 19793966]
16. Lee MJ, Lee JH, Rubinsztein DC. Tau degradation: the ubiquitin–proteasome system versus the autophagy– lysosome system. Prog Neurobiol. 2013; 105:49–59. [PubMed: 23528736]
17. Miyata Y, Li X, Lee HF, Jinwal UK, Srinivasan SR, Seguin SP, Young ZT, Brodsky JL, Dickey CA, Sun D, Gestwicki JE. Synthesis and initial evaluation of YM-08, a blood–brain barrier permeable derivative of the heat shock protein 70 (Hsp70) inhibitor MKT-077, which reduces tau levels. ACS Chem Neurosci. 2013; 4:930–939. [PubMed: 23472668]
18. Dickey CA, Kamal A, Lundgren K, Klosak N, Bailey RM, Dunmore J, Ash P, Shoraka S, Zlatkovic J, Eckman CB, Patterson C, Dickson DW, Nahman NS Jr, Hutton M, Burrows F, Petrucelli L. The high-affinity HSP90-CHIP complex recognizes and selectively degrades phosphorylated tau client proteins. J Clin Invest. 2007; 117:648–658. [PubMed: 17304350]

19. Luo W, Dou F, Rodina A, Chip S, Kim J, Zhao Q, Moulick K, Aguirre J, Wu N, Greengard P, Chiosis G. Roles of heat-shock protein 90 in maintaining and facilitating the neuro-degenerative phenotype in tauopathies. Proc Natl Acad Sci USA. 2007; 104:9511–9516. [PubMed: 17517623]
20. Erlichman C. Tanespimycin: the opportunities and challenges of targeting heat shock protein 90. Expert Opin Investig Drugs. 2009; 18:861–868.
21. Sidera K, Patsavoudi E. HSP90 inhibitors: current development and potential in cancer therapy. Recent Pat Anti-Cancer Drug Discovery. 2014; 9:1–20. [PubMed: 23312026]
22. Jhaveri K, Ochiana SO, Dunphy MP, Gerecitano JF, Corben AD, Peter RI, Janjigian YY, Gomes-DaGama EM, Koren J III, Modi S, Chiosis G. Heat shock protein 90 inhibitors in the treatment of cancer: current status and future directions. Expert Opin Invest Drugs. 2014; 23:611–628.
23. O'Leary JC III, Li Q, Marinec P, Blair LJ, Congdon EE, Johnson AG, Jinwal UK, Koren J 3rd, Jones JR, Kraft C, Peters M, Abisambra JF, Duff KE, Weeber EJ, Gestwicki JE, Dickey CA. Phenothiazine-mediated rescue of cognition in tau transgenic mice requires neuroprotection and reduced soluble tau burden. Mol Neurodegener. 2010; 5:45. [PubMed: 21040568]
24. Congdon EE, Wu JW, Myeku N, Figueroa YH, Herman M, Marinec PS, Gestwicki JE, Dickey CA, Yu WH, Duff KE. Methylthioninium chloride (methylene blue) induces autophagy and attenuates tauopathy *in vitro* and *in vivo*. Autophagy. 2012; 8:609–622. [PubMed: 22361619]
25. Rubinsztein DC. The roles of intracellular protein-degradation pathways in neurodegeneration. Nature. 2006; 443:780–786. [PubMed: 17051204]
26. Dolan PJ, Johnson GV. A caspase cleaved form of tau is preferentially degraded through the autophagy pathway. J Biol Chem. 2010; 285:21978–21987. [PubMed: 20466727]
27. Caccamo A, Majumder S, Richardson A, Strong R, Oddo S. Molecular interplay between mammalian target of rapamycin (mTOR), amyloid-beta, and Tau: effects on cognitive impairments. J Biol Chem. 2010; 285:13107–13120. [PubMed: 20178983]
28. Majumder S, Richardson A, Strong R, Oddo S. Inducing autophagy by rapamycin before, but not after, the formation of plaques and tangles ameliorates cognitive deficits. PLoS One. 2011; 6:e25416. [PubMed: 21980451]
29. Zhu XC, Yu JT, Jiang T, Tan L. Autophagy modulation for Alzheimer's disease therapy. Mol Neurobiol. 2013; 48:702–714. [PubMed: 23625314]
30. Jones JR, Lebar MD, Jinwal UK, Abisambra JF, Koren J III, Blair L, O'Leary JC, Davey Z, Trotter J, Johnson AG, Weeber E, Eckman CB, Baker BJ, Dickey CA. The diarylheptanoid (+)-a*R*,11*S*-myricanol and two flavones from bayberry (*Myrica cerifera*) destabilize the microtubule-associated protein tau. J Nat Prod. 2011; 74:38–44. [PubMed: 21141876]
31. Dai GH, Meng GM, Tong YL, Chen X, Ren ZM, Wang K, Yang F. Growth-inhibiting and apoptosis-inducing activities of myricanol from the bark of *Myrica rubra* in human lung adenocarcinoma A549 cells. Phytomedicine. 2014; 21:1490–1496. [PubMed: 24939078]
32. Whiting DA, Wood AF. Cyclisation of 1,7-diarylheptanoids through oxidative, reductive, and photochemical radical processes: total synthesies of the m,m-bridged biaryls myricanone and (±)-myricanol, and a related diarylether. Tetrahedron Lett. 1978:2335–2338.
33. Weyer, MJ.; Nye, JJ.; Ostlund, AJ.; Cook, GR. Total synthesis of the diarylheptanoid (+)-aR,11S-myricanol; 245th ACS National Meeting & Exposition; New Orleans, LA, United States. American Chemical Society; 2013. p. ORGN-182
34. Riley, AP.; Prisinzano, TE. Studies toward the total synthesis of (+)-aR,11S-myricanol; 244th ACS National Meeting & Exposition; Philadelphia, PA, United States. American Chemical Society; 2012. p. ORGN-242
35. Ogura T, Usuki T. Total synthesis of acerogenins E, G and K, and centrolobol. Tetrahedron. 2013; 69:2807–2815.
36. Semmelhack MF, Helquist P, Jones LD, Keller L, Mendelson LSR, Smith JG, Stauffer RD. Reaction of aryl and vinyl halides with zerovalent nickel–preparative aspects and the synthesis of alnusone. J Am Chem Soc. 1981; 103:6460–6471.
37. Joshi BS, Pelletier SW, Newton MG, Lee D, McGaughey GB, Puar MS. Extensive 1D, 2D NMR spectra of some [7.0]metacyclophanes and X-ray analysis of (±)-myricanol. J Nat Prod. 1996; 59:759–764.

38. Begley MJ, Campbell RVM, Crombie L, Tuck B, Whiting DA. Constitution and absolute configuration of *meta,meta*-bridged, strained biphenyls from *Myrica nagi*; X-Ray analysis of 16-bromomyricanol. J Chem Soc C. 1971:3634–3642.
39. Abisambra J, Jinwal UK, Miyata Y, Rogers J, Blair L, Li X, Seguin SP, Wang L, Jin Y, Bacon J, Brady S, Cockman M, Guidi C, Zhang J, Koren J, Young ZT, Atkins CA, Zhang B, Lawson LY, Weeber EJ, Brodsky JL, Gestwicki JE, Dickey CA. Allosteric heat shock protein 70 inhibitors rapidly rescue synaptic plasticity deficits by reducing aberrant tau. Biol Psychiatry. 2013; 74:367–374. [PubMed: 23607970]
40. Santacruz K, Lewis J, Spires T, Paulson J, Kotilinek L, Ingelsson M, Guimaraes A, DeTure M, Ramsden M, McGowan E, Forster C, Yue M, Orne J, Janus C, Mariash A, Kuskowski M, Hyman B, Hutton M, Ashe KH. Tau suppression in a neurodegenerative mouse model improves memory function. Science. 2005; 309:476–481. [PubMed: 16020737]
41. Jinwal UK, Akoury E, Abisambra JF, O'Leary JC III, Thompson AD, Blair LJ, Jin Y, Bacon J, Nordhues BA, Cockman M, Zhang J, Li P, Zhang B, Borysov S, Uversky VN, Biernat J, Mandelkow E, Gestwicki JE, Zweckstetter M, Dickey CA. Imbalance of Hsp70 family variants fosters tau accumulation. FASEB J. 2013; 27:1450–1459. [PubMed: 23271055]
42. Kruger U, Wang Y, Kumar S, Mandelkow EM. Autophagic degradation of tau in primary neurons and its enhancement by trehalose. Neurobiol Aging. 2012; 33:2291–2305. [PubMed: 22169203]
43. Caccamo A, De Pinto V, Messina A, Branca C, Oddo S. Genetic reduction of mammalian target of rapamycin ameliorates Alzheimer's disease-like cognitive and pathological deficits by restoring hippocampal gene expression signature. J Neurosci. 2014; 34:7988–7998. [PubMed: 24899720]
44. Mizushima N, Yoshimori T, Levine B. Methods in mammalian autophagy research. Cell. 2010; 140:313–326. [PubMed: 20144757]
45. Pampliega O, Orhon I, Patel B, Sridhar S, Diaz-Carretero A, Beau I, Codogno P, Satir BH, Satir P, Cuervo AM. Functional interaction between autophagy and ciliogenesis. Nature. 2013; 502:194–200. [PubMed: 24089209]
46. Abisambra JF, Jinwal UK, Blair LJ, O'Leary JC III, Li Q, Brady S, Wang L, Guidi CE, Zhang B, Nordhues BA, Cockman M, Suntharalingham A, Li P, Jin Y, Atkins CA, Dickey CA. Tau accumulation activates the unfolded protein response by impairing endoplasmic reticulum-associated degradation. J Neurosci. 2013; 33:9498–9507. [PubMed: 23719816]
47. Steelman LS, Abrams SL, Whelan J, Bertrand FE, Ludwig DE, Basecke J, Libra M, Stivala F, Milella M, Tafuri A, Lunghi P, Bonati A, Martelli AM, McCubrey JA. Contributions of the Raf/MEK/ERK, PI3K/PTEN/Akt/mTOR and Jak/STAT pathways to leukemia. Leukemia. 2008; 22:686–707. [PubMed: 18337767]
48. Sakurai N, Yaguchi Y, Hirakawa T, Nagai M, Inoue T. Two myricanol glycosides from Myrica rubra and revision of the structure of isomyricanone. Phytochemistry. 1991; 30:3077–3079.
49. Baell JB, Holloway GA. New substructure filters for removal of pan assay interference compounds (PAINS) from screening libraries and for their exclusion in bioassays. J Med Chem. 2010; 53:2719–2740. [PubMed: 20131845]
50. Chaput D, Kirouac LH, Bell-Temin H, Stevens SM Jr, Padmanabhan J. SILAC-based proteomic analysis to investigate the impact of amyloid precursor protein expression in neuronal-like B103 cells. Electrophoresis. 2012; 33:3728–3737. [PubMed: 23161580]

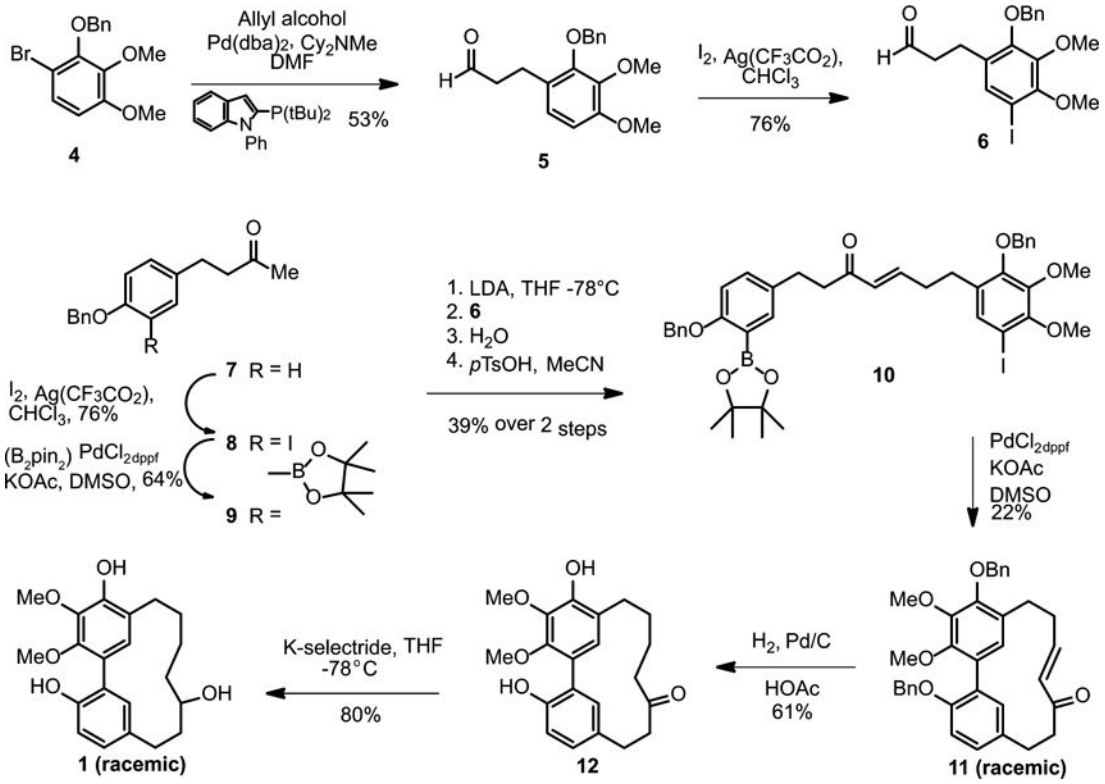


**Figure 1.**
Synthesis of **1**.

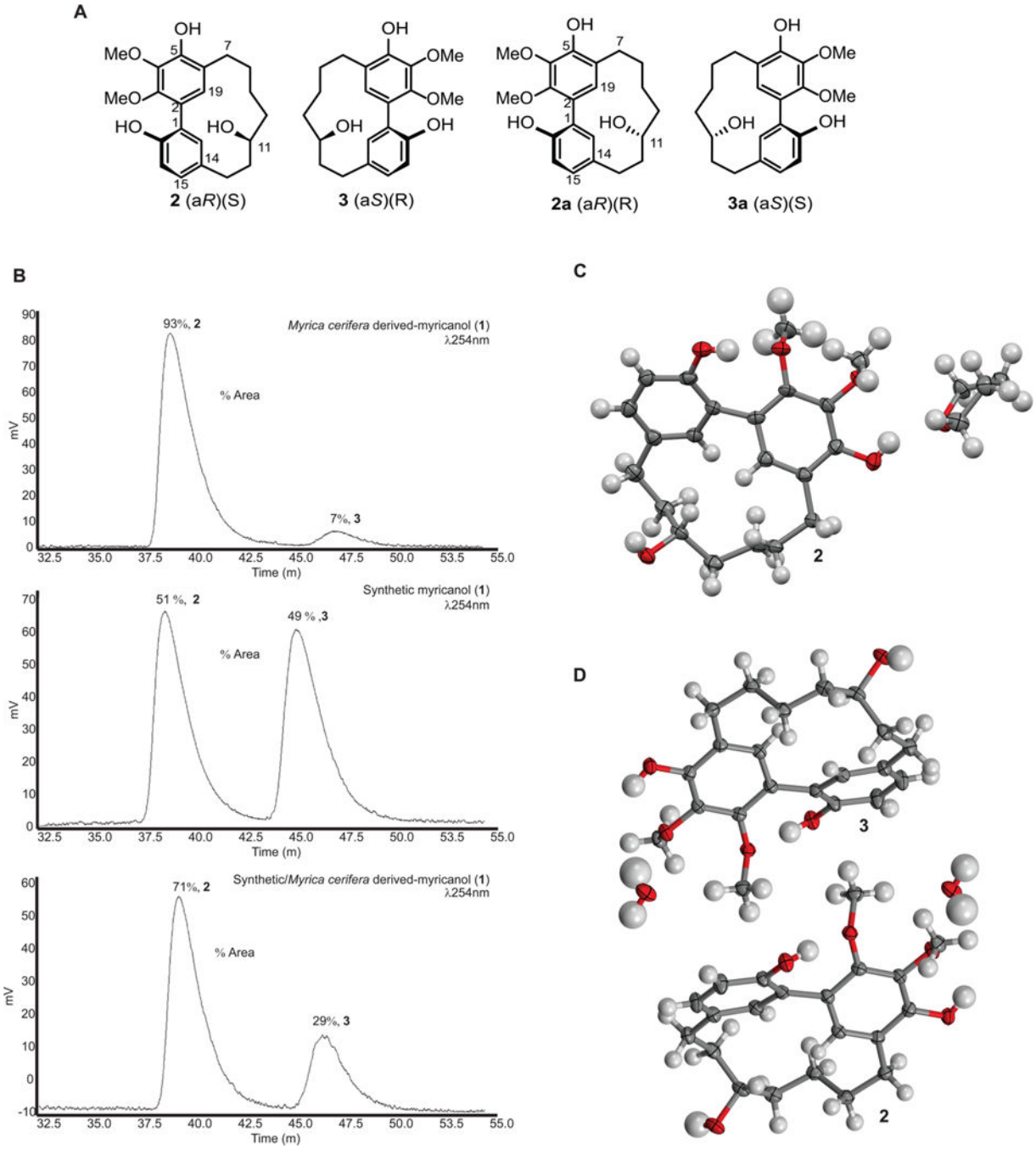


**Figure 2.**

Enantiomers of **1**. (A) Chemical structure of **1** composed of the two enantiomers, **2** and **3**, and possible atropisomers, **2a** and **3a**. (B) Chiral HPLC traces of *M. cerifera*-derived myricanol, synthetic myricanol, and *M. cerifera*-derived myricanol/synthetic myricanol (1:1) reveal 86, 2, and 42% ee, respectively. (D) The single molecule of **2** shown is a part of a large asymmetric unit containing four molecules of **2**; (D) the structure represented as a co-crystal consisted of two enantiomers, **2** and **3**, related by an inversion center; thermal

displacement ellipsoids are drawn at the 50% probability level. Coloring scheme: red, O; gray, C; and white, H.

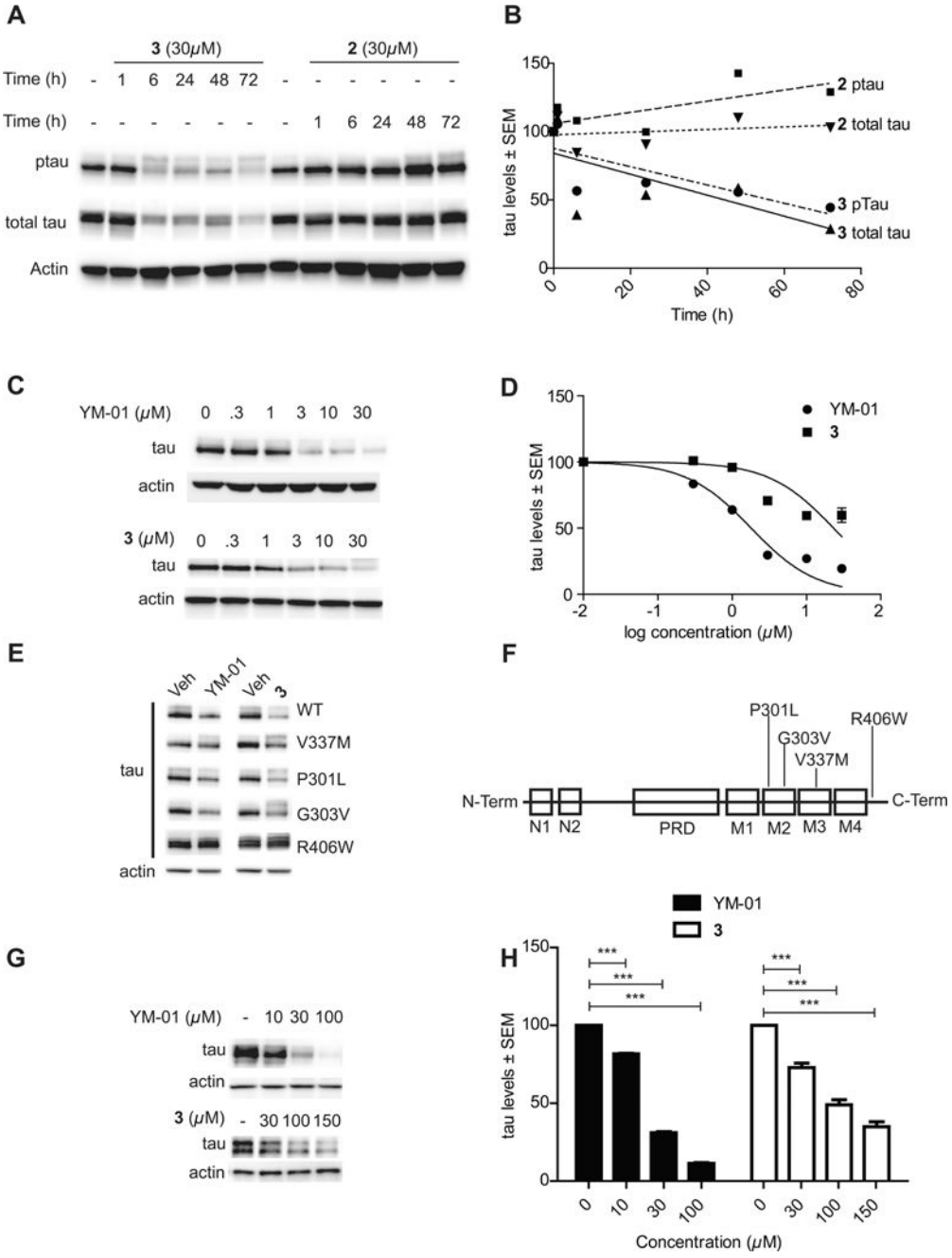


**Figure 3.**

(−)-a*S*,11*R*-Myricanol (**3**) is the enantiomer responsible for anti-tau activity. (A) Representative western blot of lysates from HEK293T cells stably overexpressing P301L tau (HEK P301L tau) treated with **2** or **3** for the indicated time. (B) Quantification of pTau (S396/404) and total tau (H150) levels from cells treated with the indicated compound and harvested at the indicated time points over 72 h. (C) Representative western blot of HEK P301L cells treated with the indicated concentrations of each compound for 24 h. (D) Half-maximal inhibitory values ($IC_{50}$) were approximately 1.8 μM for YM-01 and 18.56 μM for **3**. (E) HEK293T cells were transiently transfected with disease-causing tau mutants and

treated with $IC_{50}$ of each compound for 24 h. (F) Schematic showing location of each mutation in the tau protein. (G) Representative western blot of lysates from acute brain slices from 4 month old rTg4510 transgenic mice treated with the indicated concentrations of YM-01 or **3** for 6 h. (H) Quantification of tau levels from (G). Data are the average ± standard error of the mean (SEM); $n = 3$. Anti-tau activity of (−)-a*S*,11*R*-myricanol was observed in >10 individual experiments.

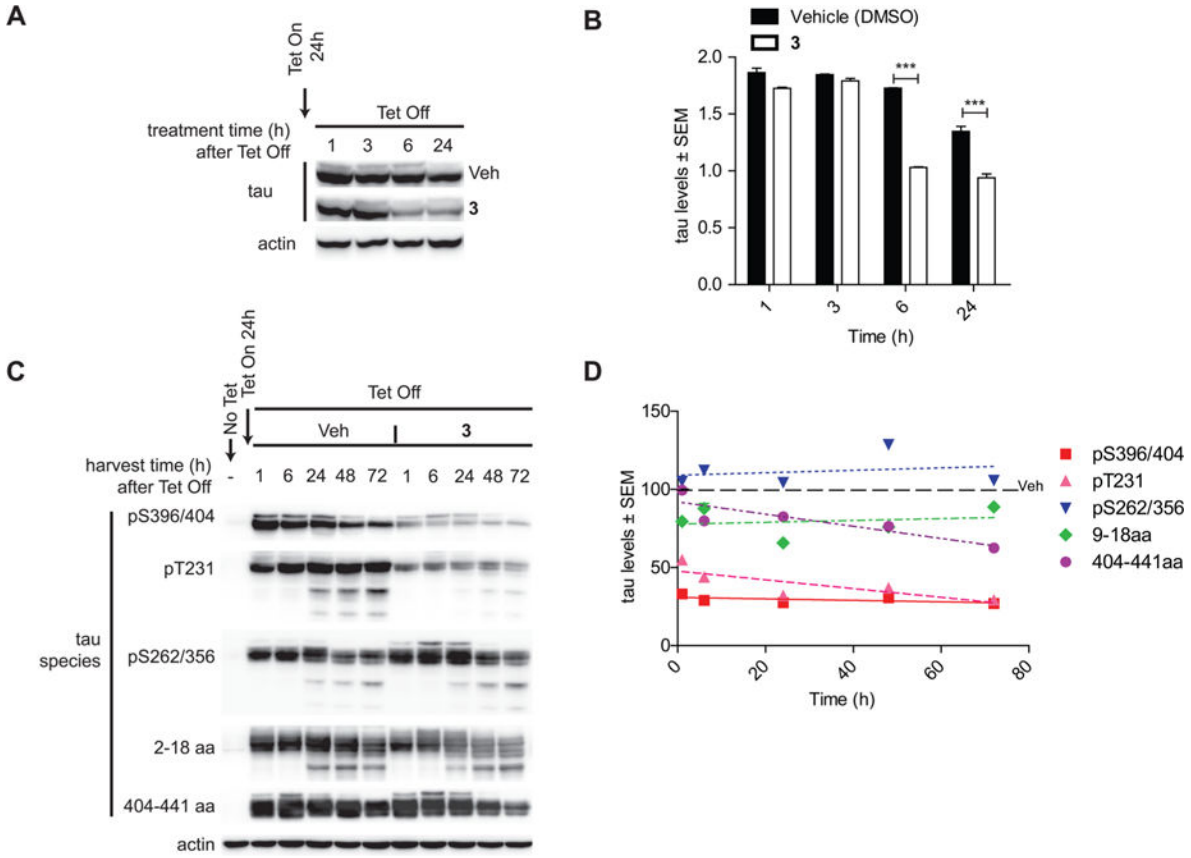


**Figure 4.**

(−)-a*S*,11*R*-Myricanol (**3**) significantly accelerates tau clearance and selectively reduces distinct tau species. (A) Representative western blot of tau levels in tet-inducible HEK293 cells stably overexpressing WT 4R0N Tau (iHEK) treated with **3** (18 μM) for the indicated time points and harvested 24 h post tetracycline removal. (B) Quantification of tau levels from (A). Data are the average ± standard error of the mean (SEM); $n = 3$. (C) Representative western blot of tau levels in iHEK cells. Expression of WT Tau was induced for 24 h with tetracycline (1 mg $mL^{-1}$). Tetracycline was removed, and cells were all treated with **3** at the same time. Lysates were harvested at the indicated time points and analyzed by western blot for levels of the indicated tau species. (D) Quantification of levels of each tau species in (C). Data are the average ± SEM; $n = 3$.

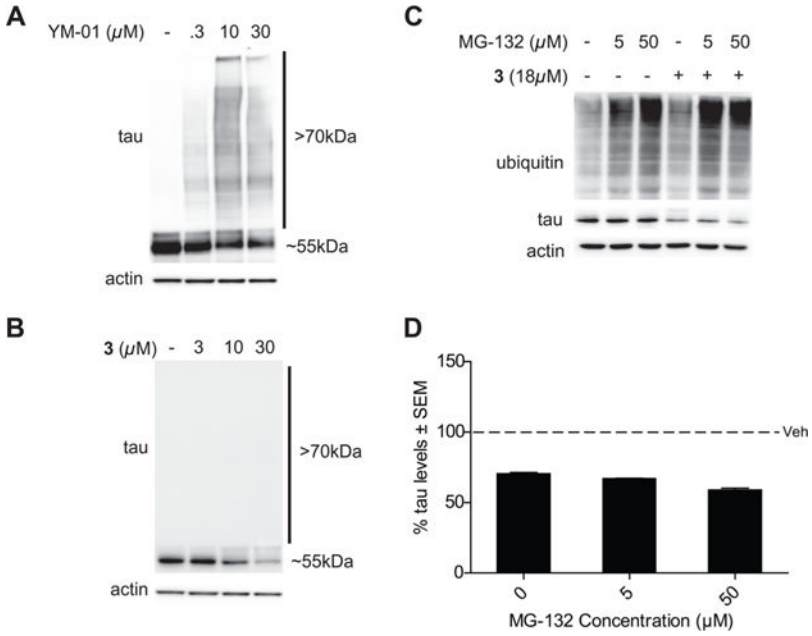


**Figure 5.**

(−)-a*S*,11*R*-Myricanol (**3**) clears tau through a non-proteasomal pathway. Representative western blot analysis of HEK293 cells transiently transfected P301L tau and treated with either YM-01 (A) or **3** (B) at the indicated concentrations for 24 h. (C) Representative western blot of lysates from HEK P301L tau cells cotreated with **3** and proteosomal inhibitor MG-132 for 4 h. (D) Quantification of tau levels in (C) as a percentage of vehicle treated ± standard error of the mean (SEM); $n = 3$.

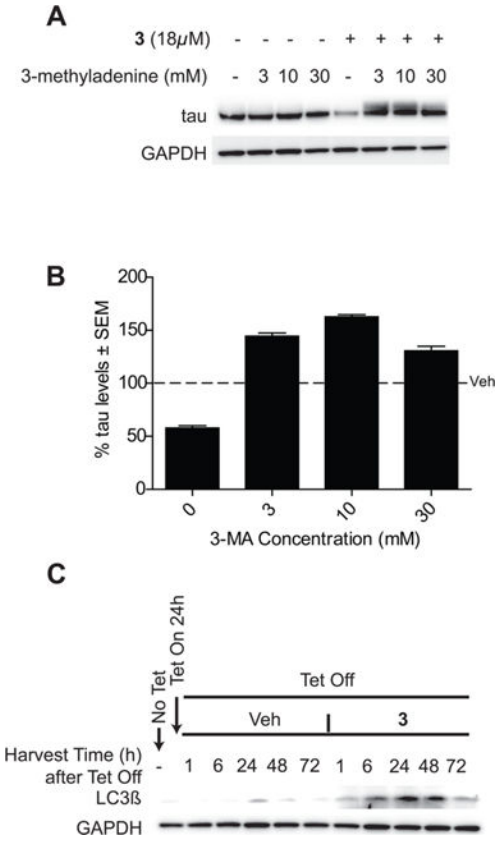


**Figure 6.**

(−)-a*S*,11*R*-Myricanol (**3**) clears tau via autophagy. (A) Representative western blot of lysates from HEK P301L tau cells cotreated with **3** and the autophagy inhibitor, 3-methyladenine (3-MA), at the indicated concentrations for 6 h. (B) Quantification of tau levels in (A) as a percentage of vehicle treated ± standard error of the mean (SEM); $n = 3$. (C) Representative western blot of LC3$\beta$ levels in iHEK cells. Expression of WT Tau was induced for 24 h with tetracycline (1 mg $mL^{-1}$). Tetracycline was removed, and cells were all treated with **3** at the same time. Lysates were harvested at the indicated time points and analyzed by western blot for levels of LC3$\beta$. Densitometric values are average ± SEM.

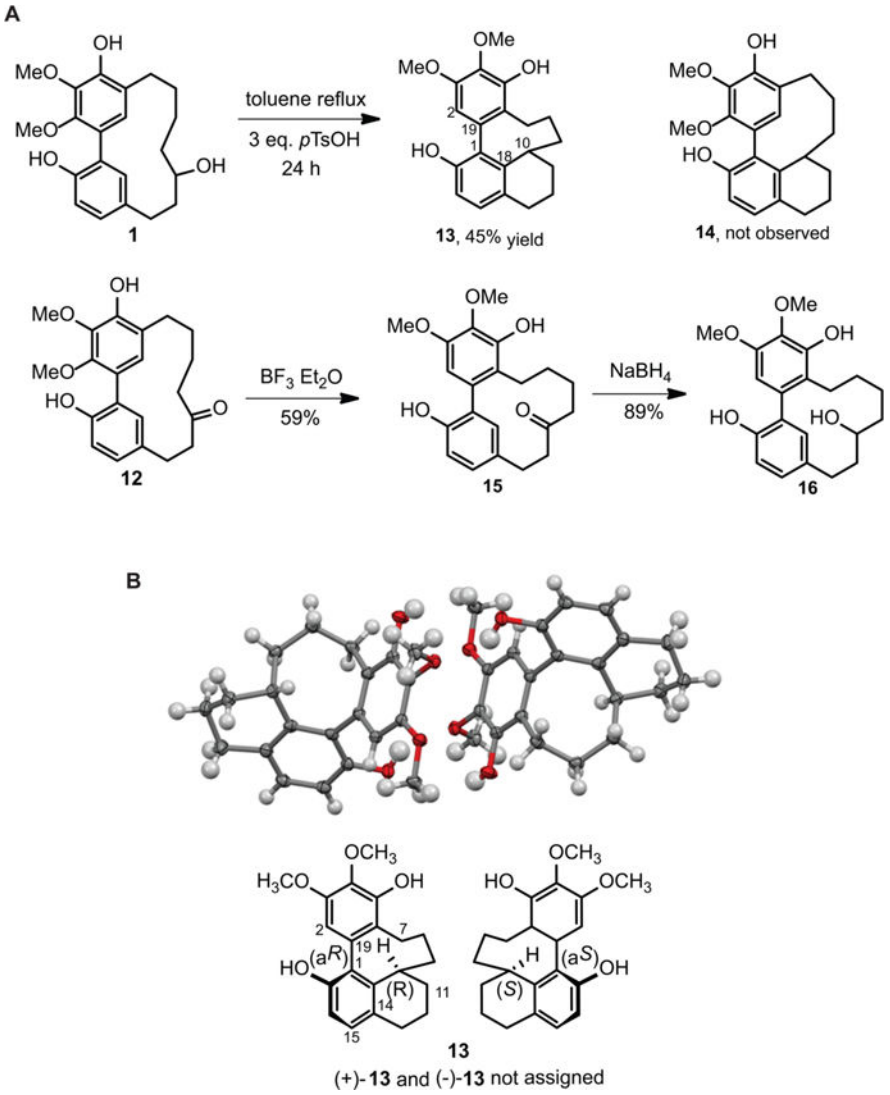


**Figure 7.**

Synthesis of **16** and a cyclized tetralin derivative thereof, **13**. (A) The acid-mediated dehydration of **1** produced cyclized tetralin **13** as the major product, in which a rearrangement occurred. Compound **15** was prepared as described and reduced to **16**. (B) The structure of **13**, represented as a co-crystal, consisted of two enantiomers related by an inversion center. Thermal displacement ellipsoids are drawn at the 50% propability level. Coloring scheme: red, O; gray, C; and white, H.

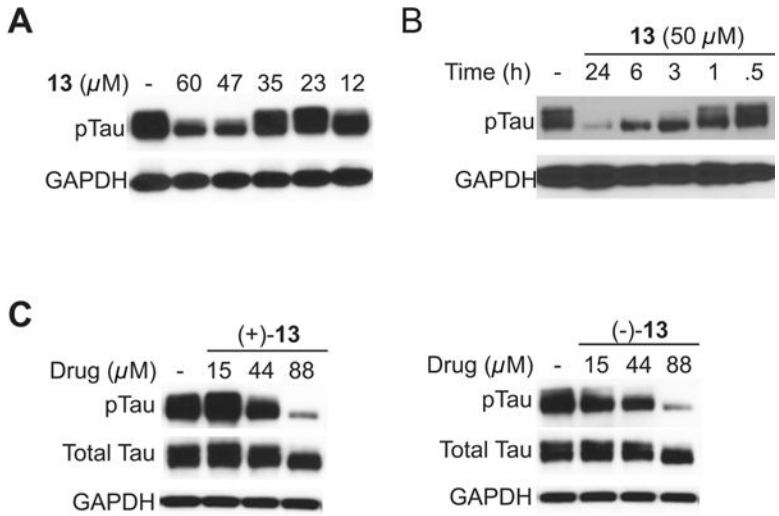


**Figure 8.**

Tau levels are decreased by **16**-like tetralin derivative **13**. (A) Representative western blot analysis of HeLa cells stably expressing 4R0N tau and treated with compound **13** at the indicated concentrations for 24 h. (B) Representative western blot analysis of HeLa tau cells and treated with compound **13** at 50 $\mu$M for indicated time points. (C) Representative western blot analysis of HeLa tau cells treated with either (+)-**13** or (−)-**13** at the indicated concentrations for 24 h.